

DESIGN OF HIGH EFFICIENT InN QUANTUM DOT BASED SOLAR CELL

M. A. A. Humayun¹ M. A. Hossain²

¹Department of EEE, Rajshahi University of Engineering & Technology, Rajshahi 6204, Bangladesh

²Department of EEE, Rajshahi University of Engineering & Technology, Rajshahi 6204, Bangladesh
humayun0403063@gmail.com¹ amzad_nam@yahoo.com²

Abstract:

A fundamental limitation in achieving ultra-high efficiency solar cells (> 50%) is the availability of materials and corresponding device structures. The InGaN material system offer substantial potential in developing ultra-high efficiency devices, both because of measurements indicating that the band gap on InN is lower than previously thought and also due to other unique material properties, such as the strong polarization and affiliation piezoelectric effects. Several key issues remain, including p-type doping, which substrates to use, and the material quality of the layers. Results show that the material quality of existing films allows a 5 stack tandem at 500X to approach 50%. Results also show InN grown on Ge with a crystalline Al interlayer, which could be used to replace a tunnel contact. High band gap GaN p-i-n and InGaN/GaN quantum dot solar cells are fabricated, showing good spectral response and Voc > 2V.

Keywords: Solar energy, High efficiency, Quantum dot, InN

1 INTRODUCTION

The theoretical efficiency limits of solar energy conversion are strongly dependant on the range and number of different band gaps or effective band gaps that can be incorporated into a solar cell. For tandem devices, the range of band gaps available as well as the ability to achieve junctions with specific band gaps and device structures is critical in achieving high efficiency. For alternate approaches, in which one or more of the band gaps are “effective band gaps” due to physical mechanisms such as an intermediate band, higher order excited states, or energy levels or bands introduced by quantum well or quantum dots, the need for specific band gaps is relaxed. However, in both approaches, both the low and the high band gaps are still controlled by the materials system. Consequently, the recent remeasurement of the band gap of InN as on the order of 0.7 eV makes the InGaN alloy system a potential solar cell material.

While band gaps figure prominently in determining efficiency limits, the ability to implement a practical, high efficiency device depends on many other parameters, including absorption, diffusion length, effect of surfaces, lattice constant, and doping. This paper determines the ability to use InGaN for photovoltaic devices with the goal of determining if the InGaN material system can be used to make ultra-high

efficiency (>50% efficiency) solar cells. The advantages of the III-nitride material system are a wide range in band gap, high absorption coefficient, a low effective mass (high mobility), and strong piezoelectric and polarization effects. However, in addition to these advantages, the material system also has significant challenges, some of which are related to the newness of the material (particularly for InN, for which photoluminescence is only measured 2 years ago [1,2,3]), including material quality, defect density, doping, substrates and growth issues.

2 MATERIAL SYSTEMS FOR ULTRA-HIGH EFFICIENCY SOLAR CELLS

The thermodynamic efficiency limits of solar energy conversion, 68.2% at one-sun and 86.8% under maximum concentration are well-known [4]. There are three sets of parameters that need to be specified: the concentration ratio, the number of band gaps or effective band gaps, and the values of the optimum band gaps. The concentration ratio is determined by taking an intermediate value between the concentration ratios at which peak solar cell efficiencies have been calculated and the value of existing concentrator modules. There are multiple reports of concentrators operating in the region of 1000X [6,7,8]. In this paper, a 500X concentration is used as an advance on 350X.

To calculate the number of band gaps or effective band gaps required in the device, detailed balance modeling [4] for devices with 4 to 8 band gaps was performed using concentration of 500X and a spectrum of 6000 K. The range of the band gaps required increases as expected with the number of band gaps (n). However, at high values of n , the lowest value of the band gap essentially saturates due to low available energy in the long wavelength region of the spectrum, and above $n = 5$ the spread in band gap is mainly accommodated by going to higher band gaps. If an AM1.5 spectrum is used rather than a black body spectrum at 6000K, the range of band gaps is narrower and the efficiency is higher, but the trends remain similar.

Once the number and values of the band gaps have been identified to achieve $> 50\%$ efficiency, the material system to most closely implement these band gaps must be determined. Fig. 1 shows the available material systems, plotting the band gap and lattice constant. Existing threejunction tandems use GaInP/GaAs/Ge or GaInP/InGaAs /Ge and have achieved efficiencies of 36.9% [5, 9]. However, above 3 junctions, achieving a lattice matched device becomes increasingly difficult. Dilute nitrides [10] and mechanical stacks using the antimonide system [11] have been proposed for 4-junction devices. Increasing the number of devices to 5-junctions will require a device with substantial lattice mismatch. In addition, the wide band gap non-nitride III-V materials are indirect and also have lower than optimum band gaps. However, one disadvantage of the III-nitrides is that they do not have a physical band gap below 0.68 eV. However, since the low band gap device in the tandem offers relatively low voltages, tandem stacks which require band gaps below 0.68 eV may be advantageously implemented by an “effective” band gap, such as quantum well or quantum dot approaches.

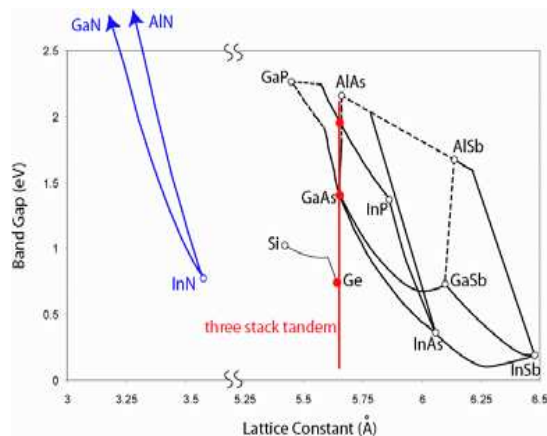


Fig. 1: Lattice-band gap diagram for III-V solar cell materials, including the III-nitrides.

In addition to the direct nature of the wide-band gap materials in the InGaN material system, the InGaN material system offers several advantages including the ability to substantially cover the required band gap range with a single alloy, the apparent insensitivity of the InGaN material system to high dislocation densities and

the polarization and piezoelectric properties of the material which introduce electric fields and surface dipoles that may counter the effect of dislocations and provide a new design parameter. The following sections examine properties of the III-N material system and how they can be used in photovoltaics.

3 III-N MATERIAL SYSTEM

The III-N material system, which includes AlN, GaN, InN and their alloys, has undergone remarkable development due to the use of GaN and InGaN for blue LEDs and laser diodes [12]. However the III-nitride materials mostly used for light emitters, GaN, AlN and $\text{In}_x\text{Ga}_{1-x}\text{N}$ with $x < 0.2$, were not used for solar cells due to their high band gap. InN seemed more promising, with a band gap of 1.9 eV, that could be a suitable candidate material for a two stack tandem on silicon [13]. However, as bright photoluminescence (PL) had at that time not yet been achieved from InN, the material quality seemed low for high efficiency photovoltaic devices.

3.1 SUBSTRATES

The III-nitrides typically crystallize in a wurtzite crystal structure, unlike Si, Ge, and GaAs which crystallize in a diamond or zinc-blend structure. Sapphire is the most commonly used substrate for the growth of wurtzite GaN. However, due to the large lattice and thermal mismatches between sapphire and III-Nitrides (16% for GaN on sapphire and 29% for InN to sapphire), epitaxial films on sapphire result in dislocation densities typically in the 10^7 - 10^{10} cm^{-2} range. Other substrates are SiC and ZnO which provide better lattice match, but nevertheless have similar dislocations densities. As an alternative to these substrates, both $\langle 111 \rangle$ oriented Si and Ge are excellent candidates for In-rich InGaN applications. Fig. 2 shows the lattice match of InN to Si and Ge, which is 7.8%, 11.3%, 17% and 20.1% for InN/Si, InN/Ge, GaN/Si, and GaN/Ge respectively. Thus, Si or Ge substrates are better lattice matched to InN than traditional GaN/Si or GaN/sapphire. Additionally, very high quality Si and Ge wafers are easily available at low cost and their conductivity allows for a vertical device design that can be contacted from the front and rear.

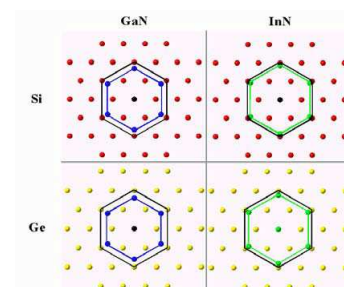


Fig. 2: Lattice structure of Si and Ge compared to InN. The Si and Ge lattice is shown as dots, with the $\langle 111 \rangle$ planes as the outer hexagonal, and GaN or InN as the inner hexagonal.

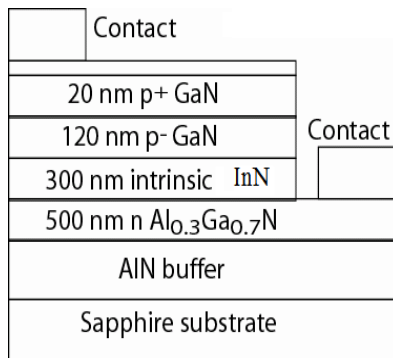


Fig. 3: Device structure of the GaN p-i-n solar cell.

3.2 POLARIZATION AND PIEZOELECTRIC CONSTANTS

In addition to its band gap range, another unique feature of the III-nitrides is the strong polarization or piezoelectric effects [14, 15]. AlN, GaN and InN are all highly polar molecules, such that at the interface between the materials, a large dipole may develop, which alters the surface properties and induces an electric field in the bulk region between two surfaces. The spontaneous polarization is particularly strong at AlN/GaN interfaces, and less so between GaN and InN. In addition to electric fields induced by polarization, an electric field may also be induced in the material by the piezoelectric fields, which are electric fields induced by strain in the material. The piezoelectric coefficients are high in the III-nitrides, hence a substantial electric field will develop in strained material. The ability to modify the surface potentials and generate electric fields across the materials is critical in the interpretation of transport properties of the III-nitrides, and is also a new design parameter [16].

3.3 P-TYPE DOPING

Achieving p-type conductivity in InGaN alloys is difficult due, in part, to a high background concentration of electrons. By improving the structural quality of GaN, p-type GaN can be achieved but one still has a limit of less than ~low to mid 10^{18} cm^{-3} hole concentration due to the deep activation energy of acceptors in GaN, which is approximately 160meV for Mg in GaN, leading to approximately 1% of the incorporated Mg contributing to the hole concentration at room temperature [17]. With InGaN, it is expected that higher hole concentrations can be achieved due to a lower activation energy than for GaN. For example, the activation energies of Mg were 141 and 80 meV for 4% and 14% In mole fraction, respectively [18]. The corresponding electrical hole concentrations are 5.3×10^{18} and $1.6 \times 10^{19} \text{ cm}^{-3}$ [18]. Despite of this advantage, practical InGaN has been shown to possess higher background electron concentrations of $\sim 10^{19} \text{ cm}^{-3}$ which compensates the holes [19]. These higher background electron

concentrations likely come from the growth on larger lattice-mismatched substrates, generating shallow donors. This feature is supported by the fact that higher hole concentrations can be tained using slower growth rates, otherwise maintaining the same growth conditions for Mg-InGaN [20]. To date, no report of p-type conductivity has been given for In $>$ ~32%, indicating that p-type InN may be a challenge to obtain.

3.4 Absorption Depth and Diffusion Length

The absorption depth ($1/\alpha$) and the diffusion length (L) are critical parameters in making high efficiency solar cells. The absorption coefficient is high in all of the InGaN range, and importantly increases rapidly near the band edge. The high absorption is a critical factor in achieving high collection since the absorption depth must be shorter than the diffusion length for high collection.

While the recombination properties of InGaN films are critical in determining the performance of photovoltaic devices, substantial variation in reported values exists in the literature, even for GaN, the best characterized of the materials. The recombination processes in the III-nitrides are controlled by several possible processes: excitonic recombination, radiative recombination, non-radiative, and recombination controlled by localization of carriers caused by phase separation in In-rich InGaN alloys. The reported values of B, the band-to-band radiative recombination coefficient, vary from 1×10^{-8} to $2.4 \times 10^{-11} \text{ cm}^3/\text{s}$, but are typically on the order 7×10^{-10} [21]. These values of the radiative lifetimes are consistent with those extracted from measurements [22]. However, films in general have a high non-radiative recombination component, and measured lifetimes are typically in the range of several hundred ps to 2 nsec [23, 24, 25]. The diffusion length depends on both the minority carrier lifetime and the diffusion coefficient. The majority carrier mobility for n-type material is measured as high as $845 \text{ cm}^2/\text{Vs}$ for thick epilayers, but only 5 for minority carrier in n-type and majority holes in p-type [26] and on the order of 500 for thinner layers. The low mobilities for minority carriers mean that most extracted diffusion lengths are between 0.2 to 0.8 μm , but several reports give measured diffusion lengths of over 1 μm , [23, 25, 27].

InN and In-rich epilayers are less well characterized than GaN, and the characterization of the material is complicated by the phase separation of InGaN layers into small, localized regions of In-rich InGaN, which act to localize carries in a similar fashion as a quantum dot. Theoretically, InN has a lower band-to-band recombination coefficient than GaN [28] as well as having higher mobilities. The higher mobilities have been experimentally verified for majority carriers, with mobilities measured of $2200 \text{ cm}^2/\text{Vs}$. For epilayers, Chen et al measure a lifetime of 300 ps and a majority carrier mobility of $1340 \text{ cm}^2/\text{Vs}$ [29].

4 MODELLING InGaN TANDEM SOLAR CELLS

A key advantage of the InGaN material system is that using a tandem (or quantum-based) device with a large number of band gaps can be grown by varying the alloy composition. However, the efficiency of the resultant device will be strongly controlled by the practical material parameters, such as diffusion length. To determine the efficiency potential of InGaN tandem solar cells, a material parameter set of the InGaN alloy was developed and used to model tandem InGaN solar cells. To determine the composition of indium in the $\text{In}_x\text{Ga}_{1-x}\text{N}$ alloy, the equation relating band gap to mole fraction x is used:

According to Vegard's law the band gap of the ternary alloy $\text{In}_{1-x}\text{Ga}_x\text{N}$ can be approximated by the parabolic form .

$$E_{g\text{InGaN}}(x) = xE_{g\text{GaN}} + (1-x)E_{g\text{InN}} - b x(1-x) \quad 1$$

Where $E_{g\text{InN}} = 0.7 \text{ eV}$, $E_{g\text{GaN}} = 3.4 \text{ eV}$ and bowing parameter $b=1.4$ (for $\text{In}_{1-x}\text{Ga}_x\text{N}$). The other material parameters are taken where possible from experimental data. The details of the material parameters set are described elsewhere, but are summarized for InN and GaN in Table 1. The absorption coefficient data was taken from.

TABLE 1: PROPERTIES OF INN AND GAN USED IN PC1D.

Parameter	GaN	InN
Band Gap	3.45 eV	0.68 eV
Electron Affinity	4.1 eV	6.4 eV
Dielectric Constant	8.9	15.3
Mobility:		
Electron	2200	1000
Hole	200	5
Lifetime:		
Electron	500 ps	1 nsec
Hole	500 ps	5 nsec
Refractive Index	2.3	2.9
Intrinsic carrier	$4.455\text{E-}11$	$5.280\text{E+}12$

Fig. 4 shows that the band gap of $\text{In}_{1-x}\text{Ga}_x\text{N}$ varies with the intrinsic molar fraction of the Ga. Similarly band gap of $\text{In}_{1-x}\text{Ga}_x\text{N}$ varies with the molar fraction of InN. So a wide range of band gap can be achieved by introducing InN in the active layer of the solar cell.

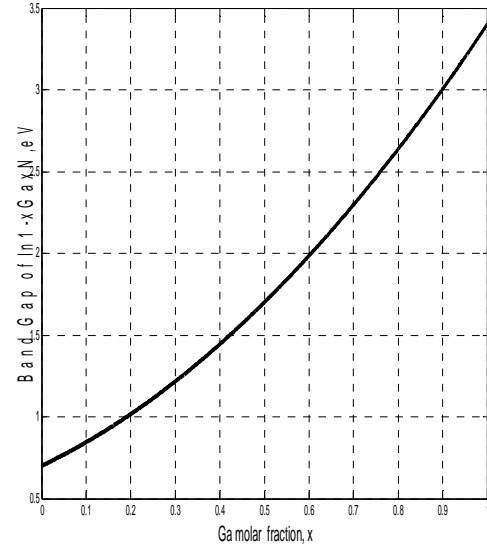


Fig. 4 Band gap energy optimization of $\text{In}_{1-x}\text{Ga}_x\text{N}$

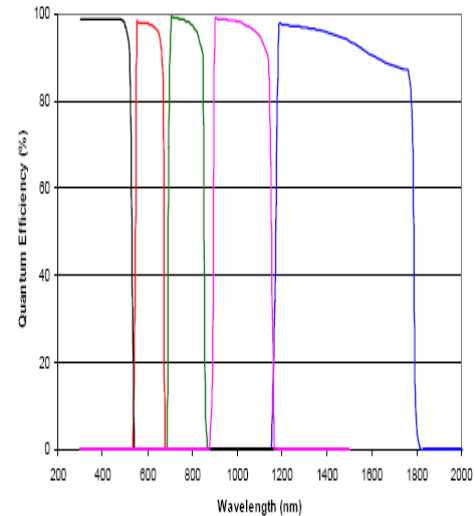


Fig. 5: QE for the 5-stack tandem from PC1D.

Fig. 5 shows the QE for a five-stack tandem made from the InGaN material system using the material parameters from Table 1 and with the reflectivity set to zero.

In addition to allowing a large range of band gaps within a single alloy system, an additional advantage of the group III nitride material is their large spontaneous and piezoelectric coefficients, giving sheet charges on the order of $1 \times 10^{13}/\text{cm}^2$, and giving an additional design parameter that can be used to mitigate the non-ideal parameters of the III-N system. For example, control over the interface charge can be used to make inversion layer devices, thus allowing solar cells without p-type doping. Using a surface charge of $-5 \times 10^{12}/\text{cm}^2$ and the parameters of Table 1 at one sun gives a solar cell with $V_{oc} = 463 \text{ mV}$, $J_{sc} = 47 \text{ mA}/\text{cm}^2$, $\eta = 14.9\%$.

The energy conversion efficiency is a key parameter in the photovoltaic solar cell technology. It is defined as

$$\eta = \frac{FFV_{OC}J_{sc}}{P_{in}} \quad 2$$

where FF is the fill factor, V_{oc} is the open circuit voltage, J_{sc} is the short-circuit current density, and P_{in} is the incident power per unit area. The performance of the conventional bulk semiconductor cells is limited to about 33%. The theoretical thermodynamic limit on the conversion of sunlight to electricity is much higher, about 93%. Thus, there is a very strong motivation for finding new approaches, which would allow one to increase the solar cell efficiency.

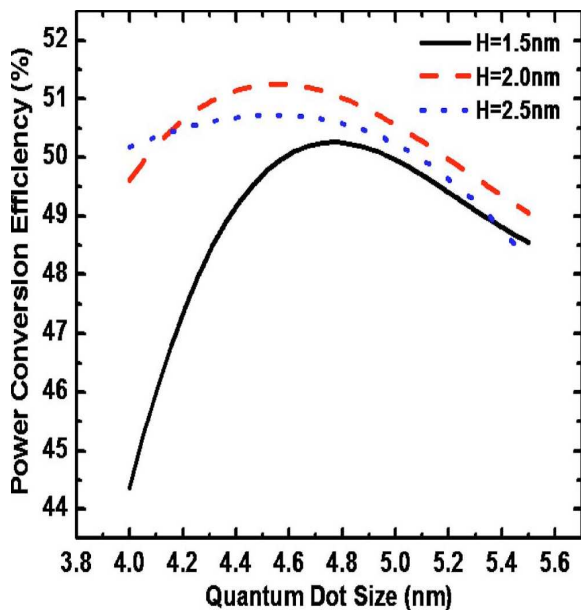


Fig. 6: Photovoltaic power conversion efficiency as a function of the quantum dot size in $\text{In}_{0.9}\text{N}_{0.1}/\text{Ga}_{0.98}\text{Sb}_{0.02}$ quantum dot supracrystal. The results are shown for several interdot separations. The inset shows the electron density of states in the miniband 111, which serves as an intermediate band in the supracrystal solar cell.

5 CONCLUSIONS

The InGaN material system has several unique properties, particularly the wide range of band gaps over the alloy composition and the polarization properties that make it suitable to ultra-high efficiency photovoltaics. Using measured material parameters where available, PC1D modeling shows that a 5-stack tandem at 500X approaches 50% efficiency. Experimental results of InN films grown on Ge show a crystalline Al interlayer, which can be used to replace tunnel junctions. Experimental results on high band gap InGaN QW solar cells (3.1 eV), show open circuit voltages of 2.1 V, and estimated external QW of > 30%.

6. REFERENCES

- [1] V. Yu. Davydov, et al., *Physical Status Solidi B*, 229, 3, p. R1-R3, (2002).
- [2] J. Wu, W. Walukiewicz, K.M. Yu, J.W. Ager, E.E. Haller, and Schaff, W.J. Hai Lu, *Applied Physics Letters*, 80, 25, p. 4741-3, (2002).
- [3] T. Matsuoka, H. Okamoto, M. Nakao, H. Harima, and E. Kurimoto, *Applied Physics Letters*, 81, 7, p. 1246-8, (2002)
- [4] A. Devos, "Endoreversible Thermodynamics of Solar Energy Conversion", OUP, 1992.
- [5] K. Emery, D.L. King, S. Igari, W. Warta, M.A. Green, *Progress in Photovoltaics*, 12, 1, 55-62, (2004).
- [6] S.R. Kurtz, and D.J. Friedman, *AIP Conference Proceedings*, 462, p. 378-84, (1999).
- [7] J.M. Gordon, E.A. Katz, D. Feuermann, and M. Huleihil, *Applied Physics Letters*, 84,18, 3642-4, (2004).
- [8] M.J. O'Neill, A.J. McDaniel, and P.A. Jaster, *Proc. 29th PVSC*, 1369-72, (2002).
- [9] R. R. King, et al, 3rd World Conference on Photovoltaic Energy Conversion, Japan, (2003).
- [10] J.F. Geisz, and D.J. Friedman, *Semiconductor Science and Technology*, 17, p. 769-777, (2002).
- [11] C. Agert, P. Lanyi, O.V. Sulima, W. Stolz, and A.W. Bett, *IEEE Proceedings-Optoelectronics*, 147, 3, p. 188-92, (2000).
- [12] S. Nakamura, S. Pearton, G. Fasol, "The blue laser diode, 2 ed", Springer Verlag 2000.
- [13] T. Yamaguchi, C. Morioka, K. Mizuo, M. Hori, T. Araki, A. Suzuki, and Y. Nanishi, 2003 International Symposium on Compound Semiconductors, 2003, p 10-11, (2003)
- [14] F. Bernardini, and V. Fiorentini, *Physical Review B*, 64, 8, 085207/1-7, (2001).
- [15] V. Fiorentini F. Bernardini, *physica status solidi (b)*, 216, 1, p. 391-398, (1999).
- [16] O. Ambacher et al., *Journal of Applied Physics*, 85, 3222 (1999).
- [17] T. Tanaka and A. Watanabe, H. Amano, Y. Kobayashi, I. Akasaki, S. Yamazaki and M. Koike, *Appl. Phys. Lett.*, 65, 5, pp. 593-594 (1994)
- [18] K. Kumakura, T. Makimoto and N. Kobayashi, *Jpn. J. Appl. Phys.* 39, 4B, pp L337-L339 (2000)
- [19] W. Geerts, J.D. Mackenzie, C.R. Abernathy, S.J. Pearton, and T. Schmiedel, *Solid- State Electronics*, 39, 9, pp 1289-1294 (1996)
- [20] K. Kumakura, T. Makimoto, and N. Kobayashi, *Journal of Crystal Growth*, 221, 267-270 (2000)
- [21] O. Brandt, H.-J. Wünsche, H. Yang, R. Klann, J.R. Müllhäuser, and K.H. Ploog, *Journal of Crystal Growth*, 189/190, 790-793, (1998).
- [22] Y. Narukawa, S. Saijou, Y. Kawakami, S. Fujita, T. Mukai, and S. Nakamura, *Applied Physics Letters*, 74, 4, p. 558-560, (1999).
- [23] A. Matoussi, et al, *phys. stat. sol. (b)* 240, 1, 160-168 (2003).
- [24] Z.Z. Bandic, P.M. Bridger, E.C. Piquette, and T.C. McGill, *Journal of Applied Physics*, 72, 24, 3166-3168, (1998).
- [25] L. Chernyak, A. Osinsky, and A. Schulte, *Solid-*

- State Electronics, 45, 9, p 1687-702, (2001).
- [26] Z.P. Gaun, J Z Li, G Y Zhang, S X Jin, and X M Ding, *Semicond. Sci. Technol.*, 15, 1, (2000) 51-54
- [27] A. Vertikov, I. Ozden, and A.V. Nurmikko, *Appl. Phys Lett.* 74 ,(6) 1999, p 850-2.
- [28] A. Dmitriev, and A. Oruzheinikov, *Journal of Applied Physics*, 86, 6, (1999), 3241.
- [29] F. Chen, A.N. Cartwright, W.J. Schaff, H. Lu, *Applied Physics Letters*, 83, 24, 4984- 6, (2003)

7. NOMENCLATURE

Symbol	Meaning	Unit
FF	fill factor	
Voc	Open circuit voltage	(mV)
Jsc	short-circuit current density	mAcm^{-2}
Pin	incident power per unit area.	mW cm^{-2}